THE JOURNAL OF PHYSICAL CHEMISTRY B

ARTICLE

pubs.acs.org/JPCB

Molecular Mobility in Solid Sodium Dodecyl Sulfate

S. Mitra,[†] V. K. Sharma,[†] V. Garcia Sakai,[‡] J. Peter Embs,[§] and R. Mukhopadhyay*[,†]

[†]Solid State Physics Division, Bhabha Atomic Research Centre, Mumbai 400085, India

[‡]Science and Technology Facilities Council, Rutherford Appleton Laboratory, Didcot, U.K.

[§]Laboratory for Neutron Scattering, Paul Scherrer Institut, Villigen, Switzerland

ABSTRACT: Here we report on the molecular mobility in solid sodium dodecyl sulfate (SDS), a commonly used surfactant, as measured by high-resolution neutron scattering in the temperature range 175−400 K. While the quasielastic data showed the presence of dynamical motion at and above 210 K, the fixed energy window (FEW) data indicated that the dynamics is present even at lower temperatures. The FEW data showed that the dynamics evolves monotonically with increasing temperature until 360 K where a dynamical transition takes place. A similar signature is also found in the differential scanning calorimetry data. The analysis of the quasielastic neutron scattering (QENS) data shows that at T < 360 K, SDS molecules undergo fractional reorientational motion about the molecular axis. With the increase in temperature the mobility progresses from the tail toward head of the molecular chain. While 11% of the molecule is mobile at 210 K, at 350 K it grows to 60% indicating a gradual melting. The same set of parameters obtained from analysis of the QENS data describes the elastic scan data as well. Above the transition, at T > 360 K, the observed dynamics correspond to localized translational diffusion of the hydrocarbon chain of the SDS molecule. It is interesting to note that the dynamical behavior of SDS in the high-temperature chain melt state is very similar to that observed for the monomer dynamics in SDS micelles.

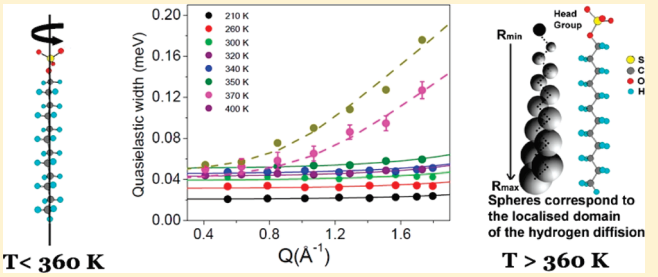

INTRODUCTION

Sodium dodecyl sulfate (SDS), $C_{12}H_{25}OSO_3^-$ Na^+, is a common surfactant used extensively in a number of applications such as cleaning agents, removal of oily stains and residues, engine degreasers, and so forth.[1] Understanding of crystal structure, phase transition and dynamical behavior are essential to facilitate the diversification of the practical usage of this surfactant molecule. Our recent neutron scattering study investigating the dynamics in SDS micellar systems at different concentrations revealed that in addition to global motion of the whole micelle, the SDS monomers undergo internal motions. While the global motion is found to follow Fickian dynamics the monomer motion is successfully described by a localized translational diffusion model in which the hydrogen atoms associated with the CH_2 units of the SDS molecular chain, diffuse inside a sphere, the radius of which increases from head toward tail with increasing diffusivity as well. It is of interest to study the dynamics of the SDS molecules in the solid phase of SDS. The crystal structure of SDS powder has been investigated in quite some detail through a combination of synchrotron, X-ray diffraction, and molecular modeling techniques.[2,3] At ambient conditions, the crystal structure of anhydrous SDS has been found to be monoclinic with a single molecule in the asymmetric unit. An electrostatic interaction between the head groups dominates the packing and largely determines the alignment of the hydrocarbon chains with respect to the long axis of the unit cell. The SDS molecules are arranged tail to tail in double layers having a tilt angle of 15° with respect to the long axis of the unit cell (Figure 1). There exists an alternating 2 Å displacement of adjacent molecules perpendicular to the layer plane due to electrostatic interactions within the polar region. This arrangement of the polar head groups determines the lateral packing of the molecules and leaves the hydrocarbon chains with about 10% larger cross sectional area than is usual in solid state chain packing arrangements.[3] This could perhaps be sufficient to introduce disorder in the conformation of the chain and permit reorientation of the hydrocarbon chains. Picquert[4] had shown the existence of rotational disorder in anhydrous SDS powder using Raman spectroscopy. Therefore it is interesting to probe this kind of disorder, which can be studied conveniently using quasielastic neutron scattering (QENS). In a QENS experiment, information on molecular dynamics is obtained by considering the dynamical structure factor, $S(\mathbf{Q},\omega)$, which indicates the probability that an incident neutron undergoes a scattering process with an atom by exchanging an amount of energy $\hbar\omega$ and momentum $\hbar\mathbf{Q}$. Characteristic times and the spatial extent of the molecular dynamics can be obtained by analyzing the ω and $\mathbf{Q}$ dependence of $S(\mathbf{Q},\omega)$ respectively.[5] We have employed the QENS technique to study a variety of organic and inorganic systems, polymer, liquid crystals, monolayer protected clusters, etc.[6−12] Dynamics in more complex systems such as phospholipid liposomes has also been studied using QENS, where it was

Received: June 2, 2011
Revised: July 19, 2011
Published: July 19, 2011

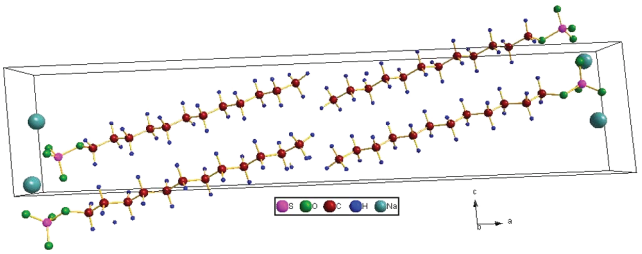

Figure 1. Unit cell of anhydrous SDS.

shown that the dynamical motion sets in the tail of the hydrocarbon chains even at temperatures much lower than the melting temperature.[13]

Here, we report on the molecular mobility in SDS powder as studied by high resolution neutron scattering in the temperature range 175−400 K.

EXPERIMENT

Sodium dodecyl sulfate (electrophoresis grade) was obtained from Sisco Research Laboratories, Mumbai, India. Neutron scattering experiments were carried out using the backscattering spectrometer IRIS at the ISIS facility, U.K., and the direct geometry spectrometer FOCUS at the Paul Scherrer Institute, Switzerland. IRIS was operated with the 002 pyrolytic graphite analyzer providing energy resolution of $\Delta E \sim 17\ \mu$eV (full width at half-maximum) and with an energy transfer range of ±0.4 meV. Data were recorded in the temperature range 210−340 K and a wavevector transfer ($\mathbf{Q}$) range of 0.5−1.8 Å^{-1}. FOCUS offers a much larger dynamical range compared to IRIS and is suitable for studying the present system at high temperatures. An incident wavelength of 5.75 Å was used for the present study to achieve an energy resolution of $\Delta E \sim 55\ \mu$eV. Data were recorded in the temperature range 300−400 K and at a wavevector transfer range of 0.4−1.73 Å^{-1}. Fixed window scans (elastic scans) were carried out as a function of temperature (in the range 175−400 K) using the IRIS spectrometer. The samples were placed in an aluminum can with sample thickness of 0.2 mm (which ensures no more than 10% scattering) such that multiple scattering effects are avoided. The ISIS data analysis package, MODES,[15] and DAVE,[16] developed by NIST, were used to carry out data reduction involving background subtraction, detector efficiency corrections etc. Differential scanning calorimetry (DSC) measurements was carried out in the temperature range 300−400 K at a heating rate of 5 K/min using a Setaram model No. DSC131 differential scanning calorimeter (Setaram, France).

RESULTS AND DISCUSSION

An SDS molecule ($C_{12}H_{25}OSO_3^-Na^+$) contains 25 protons per formula unit. Hydrogen atoms have a large incoherent neutron scattering cross section (80 barns compared to its coherent part of 1.7 barns; the total cross section for C atoms: 5.5 barns, 4.2 barns for O, 1.0 barns for S and 3.3 for Na). Therefore, the measured intensity in the neutron scattering experiment from SDS samples comes primarily from the incoherent scattering of the H atoms and can be written mathematically as

$$\frac{d^2\sigma}{\partial\omega\partial\Omega} \propto \frac{k_f}{k_i}[\sigma_{inc}S_{inc}(\mathbf{Q},\omega)] \qquad (1)$$

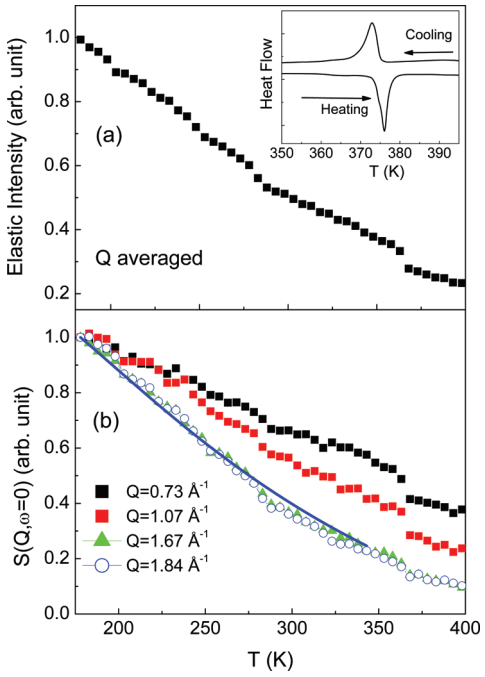

Figure 2. Temperature dependence of elastic intensity (normalized to lowest temperature studied) for (a) average over Q = 0.45 to 1.84 Å^{-1} and (b) for different Q values. The inset represents a DSC scan at 5 K/min. A melting transition is evident.

where k_f and k_i are the magnitudes of the final and initial wavevectors, σ_{inc} is the incoherent neutron scattering cross-section and $S_{inc}(\mathbf{Q},\omega)$ is the incoherent scattering law which can be written as[5]

$$S_{inc}(\mathbf{Q},\omega) = A(Q)\delta(\omega) + (1 - A(Q))L(\Gamma,\omega) \qquad (2)$$

where $A(Q)$ is the elastic fraction. The second term $(1 - A(Q))L(\Gamma,\omega)$ is the quasielastic component which appears in the spectra as a broadening of the elastic peak, where $L(\Gamma,\omega)$ is a Lorentzian function with half width at half-maximum (hwhm), Γ, which is inversely proportional to the time scale of motion, τ. The fraction of elastic contribution out of total scattered spectra is called elastic incoherent structure factor (EISF), $A(Q)$. If $I_{el}(Q)$ and $I_{qe}(Q)$ are the elastic and quasielastic intensities respectively, then EISF is defined as

$$EISF = \frac{I_{el}(Q)}{I_{el}(Q) + I_{qe}(Q)} \qquad (3)$$

EISF represents the space Fourier transform of the particle distribution, taken at infinite time and averaged over all its possible initial positions. Analysis of the EISF provides information on the geometry of the molecular motion. In the case of localized or rotational motions, the probability of finding a scatterer at infinite time within a short volume will not be zero. This contributes to the elastic component. However in the case of pure translational motion there will be no elastic component and the scattering law will have only a Lorentzian function.

Elastic scans probe the mobility in samples by determining the amount of elastic scattering as a function of temperature within the resolution of the spectrometer (∼17 μeV) used. Abrupt loss of intensity in an elastic scan experiment is an indication of a phase transition associated with a change in dynamics. Figure 2

dx.doi.org/10.1021/jp205178c |J. Phys. Chem. B 2011, 115, 9732–9738

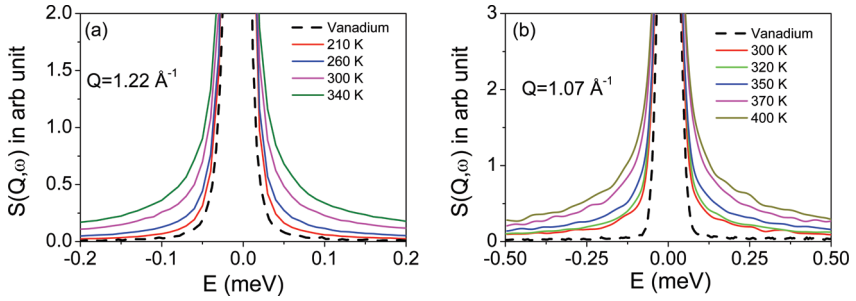

Figure 3. QENS spectra observed using (a) the IRIS and (b) the FOCUS spectrometers at different temperatures at typical Q values. Data shown are normalized to peak intensity. The instrument resolution is shown by the dashed line.

shows the elastic intensity (integrated in the energy transfer range of $\pm 10\ \mu$eV), for SDS in the temperature range 175−400 K. Figure 2a correspond to the Q averaged data for the range 0.45−1.85 Å^{-1}, normalized to the intensity at the lowest temperature. Important features observed are the monotonic decrease of elastic intensity (almost linearly) with increasing temperature up to 360 K, much more than one would have expected due to Debye−Waller factor, and a step fall in intensity is observed at 360 K indicating the existence of a dynamical transition. The monotonic decrease of intensity clearly suggests that as the temperature increases, more number of hydrogen atoms take part in the dynamics. The dynamical transition at 360 K is corroborated by the differential scanning calorimetry data where the melting transition correspond to the hydrocarbon chains is seen at ca. 375 K as shown in the inset.

The Q dependence of the elastic scans shows some interesting features as shown in Figure 2b for four typical Q values. It is found that the transition at 360 K is observed for the elastic scans for which the Q values are below a limiting Q value, $Q_{lim} \sim 1.4$ Å^{-1}, viz. 0.73 and 1.07 Å^{-1}. Transitions at 360 K are clearly present in those elastic scans for which the Q values are below Q_{lim}, while for a Q value above Q_{lim} (viz.1.67 and 1.84 Å^{-1}) the transition is not evident. This suggests that transition is observed for spatial scales above $r = 2\pi/Q_{lim} \sim 4$ Å. No transition is seen if one looks with spatial scale less than ∼4 Å. The average lateral spacing between two SDS chains is about ∼4.5 Å. It can be said that above the transition temperature, chains are dynamic over a larger spatial scale, but limited to the distance between the chain axes. In order to understand the nature of the dynamics, detail analysis of the quasielastic data is required.

Data from solid SDS as obtained from IRIS spectrometer showed significant quasielastic (QE) broadening over the resolution function of the instrument at 210 K and above. The maximum temperature was restricted to 400 K due to poor stability of the sample at higher temperatures. The observed broadening should correspond to the stochastic dynamics of the SDS molecules. Typical QENS spectra as obtained with IRIS and FOCUS spectrometers at a particular Q value at different temperatures are shown in Figure 3. The evolution of the QE spectra with temperature is found to be consistent with the elastic scan data. To proceed with the analysis, we separate the elastic and quasielastic components in the total spectra. For this the model scattering law (eq 2) was convoluted with the instrumental resolution function and the parameters $A(Q)$ and $\Gamma(Q)$ were determined by least-squares fitting with the measured data. The instrumental resolution function is obtained by recording spectra using a standard vanadium sample. Fits for some typical

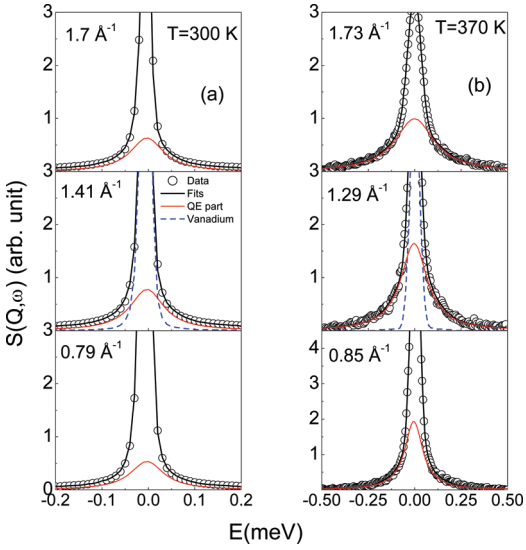

Figure 4. Typical fitted QENS spectra as observed for anhydrous SDS powder using (a) the IRIS spectrometer at 300 K and (b) the FOCUS spectrometer at 370 K at different Q values. The instrument resolution is showed by the dashed line in the middle panel.

Q values are shown in Figure 4a,b at 300 and 370 K respectively. The variation of the EISF (eq 3), $A(Q)$, as obtained from the fit, with Q, is shown in Figure 5 at different temperatures. The existence of localized dynamics in SDS is evident from the behavior of EISF. Plausible localized motions include rotation of the whole molecule or of part of the molecule, or even individual CH_2 units taking part in either diffusive or rotational motions.

Figure 5 shows that as the temperature is increased, the elastic component decreases systematically, suggesting increasing disorder in the system. Two scenarios are possible with increasing temperature: either (1) a higher proportion of CH_2 units in the hydrocarbon chains take part in the dynamics or (2) the chains become more and more flexible. Allowing for either of these possibilities, the generalized scattering law can be written as

$$S_{inc}(\mathbf{Q},\omega) = (1-p_x)\delta(\omega) + p_x[A_0(Q)\delta(\omega) + (1-A_0(Q))L(\Gamma,\omega)] \quad (4)$$

Assuming p_x to be the fraction of hydrogen atoms that are dynamically active, $(1 - p_x)$ corresponds to the immobile hydrogen atoms that would contribute toward the elastic part of the spectra. $A_0(Q)$ is the model EISF. The mobile hydrogen atoms undergoing localized motions would contribute to elastic

dx.doi.org/10.1021/jp205178c |J. Phys. Chem. B 2011, 115, 9732–9738

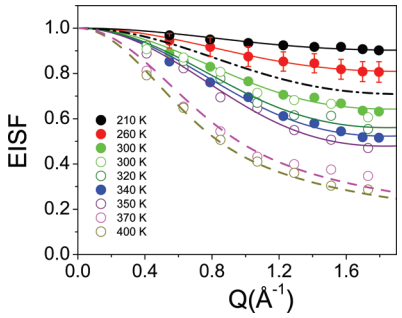

Figure 5. Variation of EISF for SDS powder with Q at different temperatures. Solid and empty circles represent data obtained with IRIS and FOCUS respectively. The solid lines represent calculated EISF for fractional uniaxial rotational diffusion model as described in text. Dashed-dotted line is for $T = 280$ K as per calculation based on fractional uniaxial rotational model (assuming $p_x = 0.33$ and $a = 1.55$ Å). Dashed lines are the fit as per localized translational diffusion model.

part weighted with $A_0(Q)$. Therefore, the total elastic fraction in the measured spectra would be, $[p_x A_0(Q) + (1 - p_x)]$.

From the geometry of the SDS molecule (Figure 1), the simplest model for chain motion is the reorientation of the chain about its own axis, known as uniaxial rotational diffusion. Considering the molecule as rigid, that is, alkyl chains are like rods and having uniaxial rotational diffusion around the molecular axis, the hydrogen atoms would rotate on a circle with a radius of rotation, a. The incoherent scattering law for a particle rotating among N equivalent sites equally distributed on a circle of radius a for a powder sample can be written as

$$S_{inc}(Q,\omega) = B_0(Qa)\delta(\omega) + \frac{1}{\pi}\sum_{n=1}^{N-1} B_n(Qa)\frac{1/\tau_n}{(1/\tau_n)^2 + \omega^2} \quad (5)$$

with

$$B_n(Qa) = \frac{1}{N}\sum_{p=1}^{N} j_0\left(2Qa\sin\frac{\pi p}{N}\right)\cos\left(\frac{2\pi np}{N}\right) \quad (6)$$

with $\tau_n^{-1} = 2\tau^{-1}\sin^2(n\pi/N)$. Here j_0 is spherical Bessel function of the zeroth order and τ is the average time spent in a site between two successive jumps. Dianoux et al.[17] showed that for $Qa \leq \pi$, the above scattering law can be used to describe the uniaxial rotational diffusion for $N \geq 6$. In that case, rotational diffusion constant, D_r can be written as

$$D_r = \frac{2}{\tau}\sin^2\left(\frac{\pi}{N}\right) \quad (7)$$

and the EISF can be written as

$$B_0(Qa) = \frac{1}{N}\sum_{p=1}^{N} j_0\left(2Qa\sin\frac{\pi p}{N}\right) \quad (8)$$

We have taken the summation for $N = 12$, a large enough number (>6) found adequate to adopt the uniaxial rotational diffusion model for the Q-range used here. After taking into account the immobile hydrogen atoms, in this case the total elastic fraction would be

$$[EISF]_{eff} = p_x B_0(Qa) + (1 - p_x) \quad (9)$$

Parameters, p_x and a are determined by least-squares fitting of the experimentally obtained EISF with this model. Fits (solid lines)

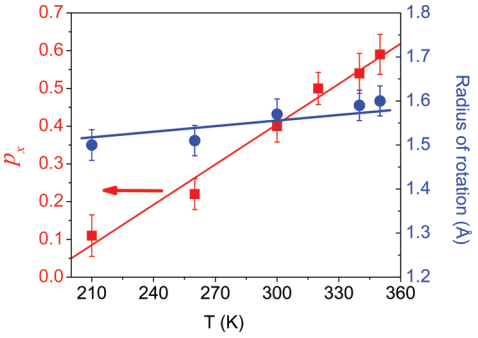

Figure 6. Variation of fractional dynamic component (p_x) of the chains and radius of rotation (a) of the chain as obtained from the least-squares fit of the EISF assuming uniaxial rotational model in the temperature range 210−350 K.

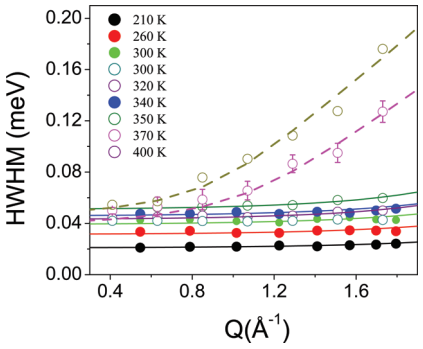

Figure 7. Variation of hwhm of a Lorentzian representing internal motion SDS powder with Q. Solid and empty circles represent data obtained with IRIS and FOCUS respectively. Solid lines are the fits with a fractional uniaxial rotational model. Dashed lines are the fit as per localized translational diffusion model.

are found to be reasonably good at all the temperatures up to 350 K as shown in Figure 5. Also apparent from the figure is an abrupt decrease in the EISF between 350 and 370 K suggesting a change in dynamic behavior. The simple model that was suitable to describe the lower temperature data is not satisfactory for $T \geq$ 370 K. This becomes more evident from the variation of the width of the QE signal, which will be discussed later.

Extracted values of p_x and a at different temperatures in the range 210−350 K are shown in Figure 6. p_x and a are found to be 0.11 (±0.05) and 1.51 (±0.04) Å, respectively, at 210 K. The value of the radius of rotation suggests that the chains are rotating around the molecular axis with a radius which is slightly more than average distance of the hydrogen atom from the molecular axis, which is 1.4 Å. This probably indicates existence of some fluctuation of the molecular axis. The value of $p_x = 0.11$ indicates that on the average only 11% of a chain is contributing to the dynamics observed at 210 K. At 350 K, values of p_x and a are found to be 0.59 (±0.06) and 1.6 (±0.05) Å, respectively. It is clear from Figure 6 that value of p_x increases monotonically, suggesting hydrogen atoms in the chains, which were earlier held fixed at low temperature, become mobile as the temperature increases. The radius of rotation, a, does not change much with increasing temperature.

The variation of the hwhm of the QE component (Γ) with Q at different temperatures is shown in Figure 7. As can be seen from the figure, the QE width (Γ) is independent of Q in the temperature range 210 to 350 K as is expected for a localized

dx.doi.org/10.1021/jp205178c |J. Phys. Chem. B 2011, 115, 9732–9738

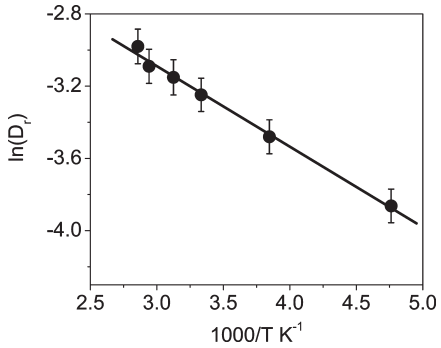

Figure 8. Variation of rotational diffusion constant in the temperature range 210−350 K. Arrhenius behavior is evident.

reorientational motion. However, at 370 K and above, the variation of the hwhm showed distinctly different behavior. Assuming a uniaxial rotational diffusion model (using eqs 5−8), the rotational diffusion constant D_r is obtained by least-squares fitting of the data in the temperature range 210−350 K. The radius of rotation a, as obtained from the EISF behavior (Figure 5), is used in the fitting procedure. Solid lines in Figure 7 show that the model provides a very good description of the experimental data. At 210 K, the rotational diffusion coefficient of SDS chain is 0.021 (±0.008) meV, which increases with temperature to 0.051 (±0.01) meV at 350 K. An increase of width with temperature suggests a faster motion or increase in diffusion constant, as expected for a thermally activated motion. The variation of rotational diffusion constant with temperature is shown in Figure 8. An activation energy of 0.9 (±0.2) kcal/mol is obtained from the Arrhenius plot of D_r in the temperature range of 210−350 K. This compares well with typical values obtained for other systems.[5]

Obtained values of p_x and activation energy can be used to describe the elastic scan data in the temperature range up to 350 K. Variation of elastic intensity obtained in an elastic scan experiment can be calculated as

$$I_{el}(\mathbf{Q}, T, \omega \approx 0) \propto \int_{-\Delta\omega}^{\Delta\omega} S(\mathbf{Q}, \omega) \otimes R(\mathbf{Q}, \omega) \mathrm{d}\omega \qquad (10)$$

$S(\mathbf{Q}\omega)$ and $R(\mathbf{Q}\omega)$ are the scattering law and instrumental resolution function respectively. $\Delta\omega$ is the hwhm of the instrumental resolution function and $\otimes$ represents a convolution product. As mentioned above, a uniaxial rotational diffusion model (eqs 5−8) is found to describe the scattering law, $S(\mathbf{Q}\omega)$ successfully. The calculated elastic intensity (shown by the solid line in Figure 2b) assuming uniaxial rotational rotational diffusion model with the same parameter set as obtained from quasielastic data analysis is found to describe the elastic scan measurement very well. Consistency of the model describing the data for two different sets of measurements is worth noting.

So far we have only discussed the data up to 350 K. At higher temperatures, both the elastic scan as well as the QENS data showed that there exists a jump in the evolution of the dynamics. The elastic scan indicated a step decrease in intensity at 360 K where as per Raman Scattering and X-ray diffraction a structural phase transition takes place. The present QENS data show a similar effect on increasing the temperature from 350 to 370 as evident in the EISF (Figure 6), which is more pronounced in the variation of hwhm (Figure 7). The model of uniaxial rotational diffusion could not describe the hwhm behavior at 370 and 400 K. Therefore, a different model beyond the scope of uniaxial rotational diffusion framework needs to be worked out. At 360 K, SDS undergoes a structural phase transition where it goes from monoclinic to hexagonal structure at high temperature.[3,4] Because of this structural transition, the lamellar thickness decreases because of the increase in tilt angle of the hydrocarbon chain with respect to long axis. An increase in tilt angle in hexagonal chain packing configurations leads to an increase in molecular area in the $a-c$ plane from 20 to 24.5 Å^2.[3] Therefore, one would expect much higher mobility due to the availability of more space since the molecular area increases by approximately >20%. It is already found that at 350 K, ∼60% of the molecules are dynamic and with the transition, it would be likely that the whole molecule would be dynamic or in other words it could be in melt state. At this stage, phenomena such as bending, stretching modes of chemical bonds, large amplitude oscillations, reorientation of SDS chain, and so forth would take place. Because of all these various motions, the hydrogen atoms of each CH_2 unit are expected to undergo diffusion but limited within a small volume of space as the crystal structure still remains intact. The shape of this volume as a first approximation may be assumed as spherical. The scattering law for diffusion of a particle within a sphere with an impermeable surface has been derived earlier by Volino and Dianoux.[18] The EISF for this model can be written as

$$EISF = A_0^0(Q) = \left[\frac{3j_1(Qa)}{Qa}\right]^2 \qquad (11)$$

where a is the radius of the sphere and j_1 is the first order spherical Bessel function. The behavior of the EISF at 370 and 400 K in Figure 5 could not be adequately described with such a model. Since the SDS chains are expected to be flexible, the hydrogen atoms associated with different carbon atoms along the chain are more likely to encompass spheres of different volumes. Therefore, we assume that hydrogen atoms belonging to different CH_2 units in the chain move within spheres of different radii. EISF curves corresponding to different hydrogen atoms can then be averaged to get the overall contribution. The distribution of radii of the spheres (within which different hydrogen atoms belonging to the different CH_2 units diffuse) can be considered to be linear where the radii of spheres increases linearly from the headgroup (SO_3 Na) toward the tail of the chains.

The resultant scattering law for such a model can be obtained by averaging the scattering laws for hydrogen atoms belonging to different CH_2 sites, generating spheres of different radii and diffusivities. The scattering law in this case can be written after modifying the Volino and Dianoux model[18] as

$$S_{inc}(Q, \omega) = \frac{1}{N}\sum_{i=1}^{N} \times \left[A_0^0(QR_i)\delta(\omega) + \frac{1}{\pi}\sum_{\{l,n\}\neq\{0,0\}}(2l+1)A_n^l(QR_i)\frac{\frac{(x_n^l)^2 D_i}{R_i^2}}{\left[\frac{(x_n^l)^2 D_i}{R_i^2}\right]^2 + \omega^2}\right] \qquad (12)$$

The first term corresponds to the elastic component while the second term is the quasielastic component, which comprises a series of Lorentzians. $A_0^0(QR_i)$ and $A_n^l(QR_i)(n,l \neq 0,0)$ are the elastic and quasielastic structure factors. $A_n^l(QR)$ for different n and l can be calculated by using the values of x_n^l listed in ref 17. R_i

Table 1. Values of the Parameters at High Temperatures As Per the Localized Translational Diffusion Model

T (K)	R_{min} (Å)	R_{max} (Å)	$D_{min} \times 10^{-5}$ (cm^2/s)	$D_{max} \times 10^{-5}$ (cm^2/s)
370	0.004 ± 0.003	3.89 ± 0.3	0.015 ± 0.005	1.78 ± 0.3
400	0.002 ± 0.001	4.44 ± 0.3	0.06 ± 0.005	2.77 ± 0.3

is the radius of the i^{th} sphere and can be expressed as

$$R_i = \frac{i-1}{N-1}[R_{max} - R_{min}] + R_{min} \quad (13)$$

D_i is the diffusivity of hydrogen atoms associated with the i^{th} site along the SDS chain and can be written as

$$D_i = \frac{i-1}{N-1}[D_{max} - D_{min}] + D_{min} \quad (14)$$

where N is total number of CH_2 units, which are taking part in the motion. In SDS ($C_{12}H_{25}OSO_3^-Na^+$), N is equal to 12. Therefore, if all the CH_2 units are taking part in the dynamics then the averaged EISF can be written as

$$A_{av}(Q) = \frac{1}{12}\sum_{i=1}^{12} A_0^0(QR_i) = \frac{1}{12}\sum_{i=1}^{12}\left[\frac{3j_1(QR_i)}{QR_i}\right]^2 \quad (15)$$

On the basis of this model, the hydrogen atoms associated with the CH_2 unit nearest to the headgroup would generate a sphere of minimum radius R_{min} having the least value of the diffusion coefficient D_{min}. And as one goes away from the headgroup along the SDS chain, both diffusivity and radius of the sphere increase and the hydrogen atoms at the end of the tail and furthest from the headgroup (the CH_3 unit) would generate a sphere of maximum radius R_{max} and associated diffusion coefficient D_{max}. The parameters R_{min} and R_{max} are obtained by least-squares fit of the experimentally obtained EISF using eq 15 (Table 1). Dashed lines in Figure 5 represent the calculation as per model discussed above. It is found that the value of R_{min} is very small while the radius of the largest sphere is about 4 Å. As we have noticed before the lateral spacing of the two SDS molecular chains is ∼4.5 Å. Our data show that at ≥370 K (chain melt state) the highest spatial extent of the molecular disorder is also of a similar value. The observed QE width has been successfully described using the same model. Since no analytical expression exists for the hwhm of the quasielastic part unlike in case of the EISF, the hwhm can be calculated numerically (using eq 12) for given values of R_{min}, R_{max}, D_{min}, and D_{max}. The least-squares fitting method is used to describe the observed QE width with D_{min} and D_{max} as parameters while the values of R_{min} and R_{max} are already known from the fit of the EISF (Figure 5). Figure 7 shows the fit of the QE widths as obtained at 370 and 400 K assuming the localized translational diffusion model to describe the dynamics of SDS in the melt state. The D_{min} and D_{max} values obtained from the fitting are given in Table 1.

We have tried to calculate the energy barrier for the rotation of the SDS molecule in the monoclinic phase of SDS. For this, a super cell of 3 × 5 × 7 unit cells was considered in which the molecule at the center of the super cell was allowed to rotate along the molecular axis keeping all others static and potential for all the non bonded interactions (both Coulombic and Lennard-Jones) are calculated in each rotational configuration. By performing this exercise, one can estimate the interaction energy on the rotating molecule due to all other SDS molecule as function of rotational angle. An attempt has also been made to relax the other SDS molecules by molecular dynamics simulation. It is found that the energy barrier for the whole molecule rotation is very high (∼400 meV), while the same for fractional dynamics is very much feasible (∼10 meV). This is in accordance to the neutron scattering data which suggested a fractional reorientation of the SDS molecule in the temperature range 175−350 K.

Results can also be compared with chain dynamics in other crystalline systems such as, monolayer-protected clusters (MPC),[6−10] liquid crystals,[11,12] dicopper tetrapalmitate,[19] phospholipid liposomes,[13] and so forth. In these systems, simple uniaxial rotational diffusion around the chain axis could not explain the experimental data. More complex motions such as uniaxial rotational diffusion of chains around the axis with additional body axis fluctuations were found to be present. For example, the dynamics of alkyl chains in Ag-based nano clusters evolve continuously with temperature. As the temperature increases, more and more hydrogen atoms contribute to the dynamics.[6] However, close to chain melting, the dynamics of alkyl chains could be best described by a model in which the hydrogen atoms undergo localized translational motions confined within spherical volumes.[10] In the case of dynamics of aliphatic chain in dicopper tetrapalmitate[19] and phospholipid liposomes,[13] a model based on localized translational diffusion explained the quasielastic data well. Like SDS, in phospholipid liposomes,[13] it was found that the hydrocarbon chains actually contribute to the observed dynamical transition. The dynamical motion in the tails of the chain starts at temperatures far below the melting transition. SDS, being a much simpler system, can thus be used as a model system to describe of evolution of chain dynamics with temperature in similar systems.

CONCLUSION

A detailed description of the reorientational motions taking place in solid SDS in the temperature range 175−400 K as studied by high-resolution neutron scattering experiments is reported. It is found that SDS molecules undergo fractional dynamics following a uniaxial rotation model in the temperature range 210−350 K and the fraction of SDS molecules taking part in the dynamics increases linearly with increasing temperature. Rotational diffusion coefficients also increase with temperature and follow Arrhenius behavior. An activation energy of 0.9 (±0.2) kcal/mol is obtained from the Arrhenius plot of D_r in the temperature range of 210−350 K for the rotational dynamics of the SDS molecule. A dynamical transition takes place at 360 K as seen in the elastic scan as well as quasielastic scattering data. Observed dynamical transition can be understood in conjunction with Raman spectroscopy and XRD studies on anhydrous SDS powder where a structural transition (from monoclinic to hexagonal) is seen around 360 K. This transition is accompanied with an increase in molecular area by 20%. Therefore, at high temperature there is more space for the chains, the chain experience a lower interaction potential and so the molecules can have more freedom to move, leading to more disorder and the resultant increase in the QE broadening in the high-temperature chain melt state. Dynamics in the chain melt state has been described by a localized translational diffusion model in which the hydrogen atoms associated with different CH_2 units of the chain diffuse within spheres of varying radii. The radii are largest at the tail end while they are smallest toward the head. Diffusivities associated with the different radii also increase from head to tail.

It is interesting to compare the results from this work of anhydrous SDS to the dynamical behavior of SDS micelles in solution as studied by QENS recently[14] by us. It was found that uniaxial rotation was inadequate to explain the internal motion of the SDS micelles. In the case of SDS micelles, it is found that the hydrogen atoms undergo localized translational diffusion confined within spherical volumes. It is worthy to note that dynamics of SDS chain in anhydrous powder at chain melt state (>360 K) is more or less similar to that in the micellar phase. Complete evolution of chain dynamics with hydration has been studied in various proteins namely lysozyme, myglobin.[20] It has been found that not only nature of motion but also time scale of motion changes with hydration from dry powder to protein solutions. We had studied the dynamics of SDS at two extreme ends; as anhydrous SDS powder and in SDS micellar solution in detail. To gather a valuable insight in understanding the evolution of chain dynamics from dry SDS powder to micellar solution, further experiments on SDS with different degree of hydration are planned.

AUTHOR INFORMATION

Corresponding Author

*E-mail: mukhop@barc.gov.in. Tel: +91-22-25594667. FAX: +91-22-25505151.

ACKNOWLEDGMENT

We acknowledge Dr. P. A. Hassan, Chemistry Division, Bhabha Atomic Research Centre, for fruitful discussion. Financial support received from the Department of Science and Technology, India is gratefully acknowledged.

REFERENCES

(1) Kwak, J. C. T. *Polymer-Surfactant Systems*; Marcel Dekkar: New York, 1998.
(2) Smith, L. A.; Hammond, R. B.; Roberts, K. J.; Machin, D.; McLeod, G. *J. Mol. Struct.* **2000**, *554*, 173–182.
(3) Sundell, S. *Acta Chem. Scand.* **1977**, *31*, 799–807.
(4) Picquart, M. *J. Phys. Chem.* **1986**, *90*, 243–250.
(5) Bée, M. *Quasielastic Neutron Scattering*, Adam Hilger: Bristol, 1988.
(6) Mukhopadhyay, R.; Mitra, S.; Johnson, M.; Rajeev Kumar, V. R.; Pradeep, T. *Phys. Rev. B* **2007**, *75*, 075414–8.
(7) Mukhopadhyay, R.; Mitra, S.; Pradeep, T.; Tsukushi, I.; Ikeda, S. *J. Chem. Phys.* **2003**, *118*, 4614–4619.
(8) Mitra, S.; Nair, B.; Pradeep, T.; Goyal, P. S; Mukhopadhyay, R. *J. Phys. Chem. B* **2002**, *106*, 3960–3967.
(9) Mukhopadhyay, R.; Mitra, S.; Senthil Kumar, P.; Tsukushi, I.; Ikeda, S. *Appl. Phys. A* **2002**, *74*, S1311–S1313.
(10) Mitra, S.; Sharma, V. K.; Pradeep, T.; Johnson, M.; Mukhopadhyay, R. *AIP Conf. Proc.* **2010**, *1313*, 292–294.
(11) Gautam, S.; Choudhury, R. R.; Panicker, Lata; Mitra, S.; Mukhopadhyay, R. *Chem. Phys. Lett.* **2008**, *453*, 207–211.
(12) Mitra, S.; Venu, K.; Tsukushi, I.; Ikeda, S.; Mukhopadhyay, R. *Phy. Rev. E* **2004**, *69*, 061709–8.
(13) Doxastakis, M.; Garcia Sakai, V.; Ohtake, S.; Maranas, J. K.; de Pablo, J. J. *Biophys. J.* **2007**, *92*, 147–161.
(14) Sharma, V. K.; Mitra, S.; Verma, G.; Hassan, P. A.; Garcia Sakai, V.; Mukhopadhyay, R. *J. Phys. Chem. B* **2010**, *114*, 17049–17056.
(15) http://www.isis.stfc.ac.uk/instruments/iris/data-analysis/modes-v3-user-guide-6962.pdf. (accessed July 23, 2011).
(16) Azuah, R. T.; Kneller, L. R.; Qiu, Y.; Tregenna-Piggott, P. L.W.; Brown, C. M.; Copley, J. R. D.; Dimeo, R. M. *J. Res. Natl. Inst. Stand. Technol.* **2009**, *114*, 341–358.
(17) Dianoux, A. J.; Volino, F.; Hervet, H. *Mol. Phys.* **1975**, *30*, 1181–1194.
(18) Volino, F.; Dianoux, A. J. *Mol. Phys.* **1980**, *41*, 271–279.
(19) Carpentier, L.; Bée, M.; Giroud-Godquin, A. M.; Maldivi, P.; Marchon, J. C. *Mol. Phys.* **1989**, *68*, 1367–1378.
(20) Perez, J.; Zanotti, J. M.; Durand, D. *Biophys. J.* **1999**, *77*, 454–469.